JOURNAL OF MATERIALS SCIENCE: MATERIALS IN MEDICINE 6 (1995) 150–154

^{19}F and ^{31}P NMR spectroscopy of calcium apatites

M. BRAUN, P. HARTMANN
Institut für Optik und Quantenelektronik, Friedrich-Schiller-Universität Jena, Max-Wien-Platz 1, 07743-Jena, Germany

C. JANA
Otto-Schott-Institut, Friedrich-Schiller-Universität Jena, Fraunhoferstrasse 6, 07743-Jena, Germany

Glass ceramics that include apatite crystals are used as implant materials. Because most of these glass ceramics are comprised of fluoride-containing glass compositions, the included apatites could be hydroxyapatite, fluorapatite or fluoride-substituted hydroxyapatite. However, these apatites differ in regard to their solubility and thermal stability. The purpose of the current study was to determine the possibilities of distinguishing between these apatities. High resolution solid-state ^{19}F and ^{31}P magic angle spinning (MAS) nuclear magnetic resonance (NMR) spectra of two fluorapatites, a hydroxyapatite and a fluoridated hydroxyapatite have been obtained. Using ^{31}P NMR investigations it is possible to distinguish between calcium apatites and other calcium phosphates, but the distinction between fluoride-containing apatite and hydroxyapatite is not possible. However, ^{19}F high-resolution solid-state NMR investigations permit the distinction between these various apatites. The results of the NMR investigations could be used for the characterization of glass ceramics. The application of those results was demonstrated using a newly developed apatite-containing glass ceramic.

1. Introduction

Nowadays in modern medicine, different implant materials are used to preserve and restore bodily functions: metals and alloys, organic polymers, glasses, glass ceramics, sinter ceramics and glass carbon. The application of bioactive materials, such as tricalciumphosphate, tetracalciumphosphate, hydroxyapatite, fluorapatite, bioglasses and glass ceramics is a growing trend. If implanted into a bone defect, a bioactive material is not encapsulated by a connective tissue, but comes into direct contact with the surrounding bone and forms a tight chemical bond with it [1]. Some different kinds of glasses and glass ceramics showing bioactive behaviour have been developed [2]. Most of the bioactive glass ceramics available today include calcium apatite as crystalline phase. Since these glass ceramics are comprised of fluoride-containing glass compositions, the precipitated apatite could be fluorapatite, hydroxyapatite or fluoride-substituted hydroxyapatite. The distinction between these kinds of apatites is a difficult problem because the crystals are relatively small and surrounded by a glassy matrix (and possibly by additional crystal phases as well). It is often impossible to distinguish definitely between fluorapatite and hydroxyapatite using X-ray diffraction, as the patterns of these apatites are very similar. However, in aqueous solutions the solubility of fluorapatite is lower than that of hydroxyapatite, which is interesting for application as a long-term stable implant. It is known that in the case of fluoridated hydroxyapatites, the solubility decreases with increasing fluoride content [3]. Furthermore, other studies have shown fluorapatite to be biocompatible with soft and hard tissue [4, 5] and it has been reported that fluorapatite is stable with respect to high temperatures (plasma-spray temperatures) [6]. That is why fluorapatite and fluorapatite-containing materials are more suited as coatings of metallic implants than hydroxyapatite or hydroxyapatite-containing bulk materials [7, 8].

In this study, the possibilities of distinguishing between fluorapatite, hydroxyapatite and fluoridated hydroxyapatite using high-resolution solid-state NMR have been determined. The results will then be applied to a newly developed apatite glass ceramic. For that purpose ^{31}P and ^{19}F MAS NMR investigations have been performed to study different mineral and synthetic apatites in the same way as an apatite-containing glass ceramic.

2. Experimental procedures

The NMR spectra were acquired on a commercial Bruker AMX 400 NMR spectrometer and a home-built solid-state spectrometer completed with a super conducting solenoid (Oxford Instr. $B_0 = 6.35$ T) operating at 109.3 MHz for ^{31}P and 254.0 MHz for ^{19}F.

0957–4530

All ^{31}P isotropic chemical shift parameters δ_{iso} and relative line intensities were obtained from high-speed MAS spectra using spinning speeds of about 13 kHz. The anisotropy ($\Delta\delta$) and asymmetry (η) parameters were obtained from the low spinning speed (about 2 kHz for ^{31}P and 4 kHz for ^{19}F) MAS spectra using the method of Herzfeld and Berger [9, 10]. The chemical shift refers to 85% solution of phosphoric acid for the ^{31}P resonance and C_6F_6 for the ^{19}F resonance.

A commercial hydroxyapatite powder (< 45 µm) supplied by MERCK (Darmstadt, FRG) is compared with a synthetic fluoridated hydroxyapatite, a natural mineral fluorapatite from Ehrenfriedersdorf (FRG) and a fluorapatite that was synthesized by a solid-state method (2 h at 1000 °C) [11]. The solid-state synthesis is based on the reaction

$$9Ca(PO_3)_2 + 11CaF_2 \rightarrow 2Ca_{10}(PO_4)_6F_2 + 6POF_3$$

The fluoridated hydroxyapatite was prepared in an aqueous medium by means of a cyclic pH variation technique described by Duff [12] in relation to the synthesis of fluorapatite. 10 g of a fresh calcium hydroxyapatite was placed in a polyethylene bottle with 500 ml of a 0.01 M aqueous solution of NaF. This system was equilibrated to pH = 7 overnight, then the pH was dropped to 4 with 1 M HNO_3. After 30 min of equilibration the pH was raised to 7 using 1 M NaOH. This cycle of pH fluctuation was repeated three times. Then the solid phase was filtered, washed with distilled water, dried at 100 °C and heat-treated at 1100 °C for 2 h.

The X-ray diffraction patterns of the solid product agree with those of crystalline calcium apatites. The fluoride content (expressed as fluoride at %, where 100 at % corresponds to the total substitution of F^- for OH^-) was determined using the method reported by Pietzka and Ehrlich [13] to be 25 at %. So the fluoridated hydroxyapatite can be described with the formula $Ca_{10}(PO_4)_6F_{0.5}(OH)_{1.5}$.

3. Results and discussion

The high-resolution solid-state NMR is of significant structural sensitivity. As seen in the case of the present ^{31}P NMR investigations, the application of correlations between the anisotropic chemical shift and structural features permits analysis of short-range structure around the nucleus under investigation.

In the case of phosphorus-containing solids such as glasses and ceramics, the ^{31}P chemical shielding is anisotropic and is described by a tensor δ. If δ_{ii} ($i = 1$, 2 or 3) are the components in the direction of the principal axes of the tensor of a given nucleus in the molecular framework, the isotropic value δ_{iso}, the shift anisotropy $\Delta\delta$ and the asymmetry parameter η can be derived according to the following relations [14]:

$$\text{isotropic shift:} \quad \delta_{iso} = \tfrac{1}{3}(\delta_{11} + \delta_{22} + \delta_{33}) \qquad (1)$$

$$\text{anisotropy:} \quad \Delta\delta = \delta_{33} - \tfrac{1}{2}(\delta_{11} + \delta_{22}) \qquad (2)$$

$$\text{asymmetry:} \quad \eta = \frac{\delta_{11} - \delta_{22}}{\delta_{33} - \delta_{iso}} \qquad (3)$$

with $|\delta_{11} - \delta_{iso}| \leq |\delta_{22} - \delta_{iso}| \leq |\delta_{33} - \delta_{iso}|$

From the literature [15–19], it is well known that structural units of different degrees of condensation (Q^n-groups, where n is the number of bridging oxygen atoms between PO_4-tetrahedra) in solid phosphates, either crystalline or amorphous, give different values of the ^{31}P chemical shift anisotropy.

In addition to this, the isotropic chemical shift correlates with the field strength of the cations surrounding the phosphate anions. As a result, the isotropic chemical shift parameters are very suitable in identifying the cation's influence on the PO_4-tetrahedra. By analysis of the MAS linewidth, it is possible to obtain information about the state of order of the materials investigated, because the MAS linewidths of amorphous (approximately 10 ppm) and crystalline (approximately 1 ppm) phases differ by a factor of ten.

The ^{31}P NMR spectra of the hydroxyapatite and fluorapatites under investigation, whether natural or synthetic, show three spectral components with significantly different relative intensities (Figs 1 and 2).

Regarding the ^{31}P shift anisotropy (using a spinning speed of 2 kHz) and the isotropic chemical shift (using a spinning speed of 13 kHz), the line B with maximum intensity of about 97% in all cases belongs definitely to crystalline apatite. Additional signals at $\delta_{iso} = 5.1$ ppm (A) and $\delta_{iso} = 0.0$ ppm (C) could be caused by tricalciumphosphate impurities (Fig. 1).

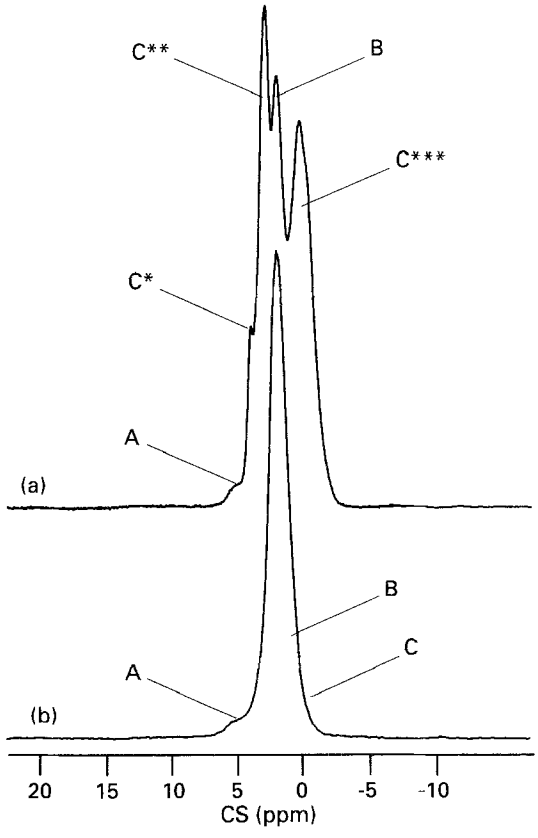

Figure 1 ^{31}P MAS NMR (sample spinning speed = 13 kHz; $B_0 = 9.39$ T) spectra of synthetic hydroxyapatite (HAp) with (a) and without (b) heat treatment 5 h 1550 °C. The main line B belongs to calciumapatite. The lines A and C correspond to β-tricalciumphosphate and α-tricalciumphosphate, respectively. The lines C*, C** and C*** represent different crystallographic phosphorus positions of α-tricalciumphosphate (seen only in samples with a relatively high content of α-tricalciumphosphate).

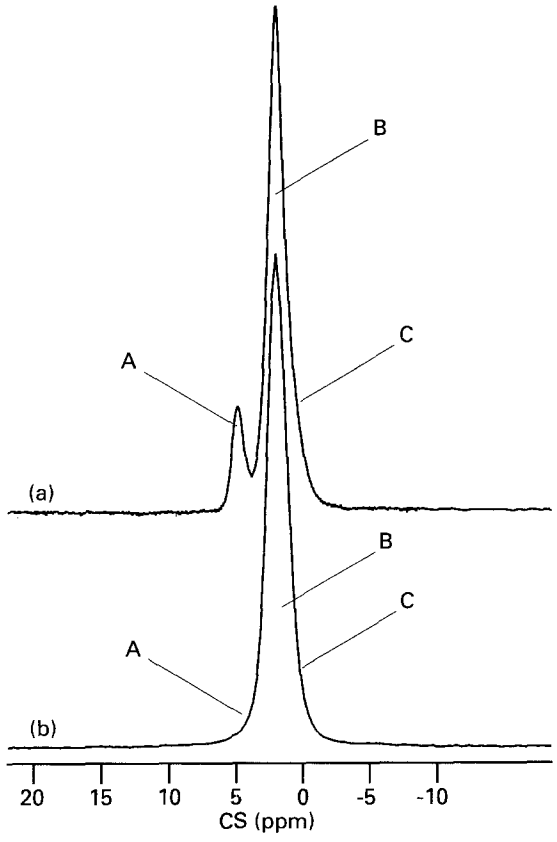

Figure 2 ^{31}P MAS NMR (sample spinning speed = 13 kHz; B_0 = 9.39 T) spectra of synthetic fluorapatite (FAp) with (a) and without (b) heat treatment 5 h 1550 °C (lines A, B and C: see Fig. 1).

The NMR spectra of crystalline apatites after heat treatment (5 h at 1550 °C) exhibit significantly higher relative intensities of the additional lines A and C. In these cases, the ^{31}P chemical shift tensor parameters obtained permit a correct attribution of the additional lines A and C to the signals of β-$Ca_3(PO_4)_3$ and α-$Ca_3(PO_4)_3$, respectively.

Both heat-treated fluorapatites exhibit fractions of tricalciumphosphate of about 10% (Fig. 2), whereas the heat-treated hydroxyapatite contains more than 90% of tricalciumphosphate (Fig. 1). This result is in agreement with the X-ray data on these materials, and the well-known solid-state reaction of the apatites to tricalciumphosphate [20]. Furthermore, the higher stability of the fluorapatites against conversion into tricalciumphosphate is confirmed. The extra signals (A and C) in the spectra of basic apatites are also caused by tricalciumphosphate.

Table I contains the ^{31}P chemical shift tensor parameters of all apatites investigated. The ^{31}P MAS NMR spectra exhibit NMR parameters that are consistently within the margin of error. The main line (apatite line) in all samples belongs definitely to isolated phosphate groups (Q^0) influenced by Ca^{2+} cations but is clearly different from those of tricalciumphosphate. In summary, it can be confirmed that ^{31}P high-resolution NMR permits clear identification of apatites in phosphate-containing solids such as glasses and ceramics. However, the distinction between fluorapatite and hydroxyapatite, using solely ^{31}P NMR, cannot be made.

TABLE I ^{31}P chemical shift tensor parameters and fractions of phosphorus in the apatite line related to total phosphorus amount in the hydroxyapatite (HAp), fluorapatites (FAp) and fluoridated hydroxyapatite (FHAp) samples investigated

Sample	δ_{iso} (ppm)	$\Delta\delta$ (ppm)	η	Relative apatite fraction (%)
Synthetic FAp	2.3 ± 0.3	32 ± 5	0.4 ± 0.2	98 ± 1
Mineral FAp	2.3 ± 0.3	27 ± 5	0.5 ± 0.2	97 ± 1
Synthetic HAp	2.3 ± 0.3	29 ± 5	0.3 ± 0.2	98 ± 1
Synthetic FHAp	2.3 ± 0.3	29 ± 5	0.3 ± 0.2	98 ± 1

The reason for this is that the structural similarity between hydroxyapatite and fluorapatite, in regard to the investigated phosphorus nucleus, is very high. Hydroxyapatite and fluorapatite crystallize in the hexagonal system in the space group $P6_3/m$ and have been reported in detail [21–23]. Both structures have high similarity, but they differ in the position of the OH^- and F^- ions. In fluorapatite, the F^- ions are located just in the centre of a triangle formed by three Ca^{2+} ions of the screw axis on the mirror planes at $z = \frac{1}{4}$ and again at $z = \frac{3}{4}$ (position of the F^- ions: 0;0; $\frac{1}{4}$ and 0;0; $\frac{3}{4}$), while in hydroxyapatite the O of the OH^- groups is located about 0.03 nm above or below the Ca^{2+} triangle. By that the O–H direction always points away from the mirror planes at $z = \frac{1}{4}$ and $z = \frac{3}{4}$.

^{19}F MAS NMR investigations promise correct identification of fluorapatite and partially fluoride-substituted hydroxyapatite. Fig. 3 shows the ^{19}F MAS NMR spectra of synthetic fluorapatite whereas Table II contains the corresponding ^{19}F shift parameters. The ^{19}F MAS NMR spectra of all fluorapatites consist of one line group. The isotropic ^{19}F chemical shifts for fluorapatites and the fluoridated hydroxyapatite differ by about 2 ppm, whereas the ^{19}F anisotropies are constant within the margin errors. The measured differences in the ^{19}F isotropic chemical shift remains representative for the deviations in the fluorine short-range structure of fluorapatites and the fluoridated hydroxyapatite. Possibly the ^{19}F isotropic chemical shift of fluoridated hydroxyapatites correlates to the relative fluorine content. Differences in the ^{19}F chemical shift asymmetries do not seem to be useful to characterize fluorine short-range structure.

Using the example of bioglass ceramics, the application of these results can be demonstrated. The focus is on a new apatite-containing glass ceramic developed in the system SiO_2–Al_2O_3–CaO–P_2O_5–Na_2O–F^- [24]. The glasses were melted at 1550 °C in a platinum crucible. The melt was poured into a preheated metal mould and was cooled to room temperature. These base glasses showed glass-in-glass phase separation, where droplets were embedded in the glass matrix. During a subsequent thermal treatment (1 h at 900 °C)

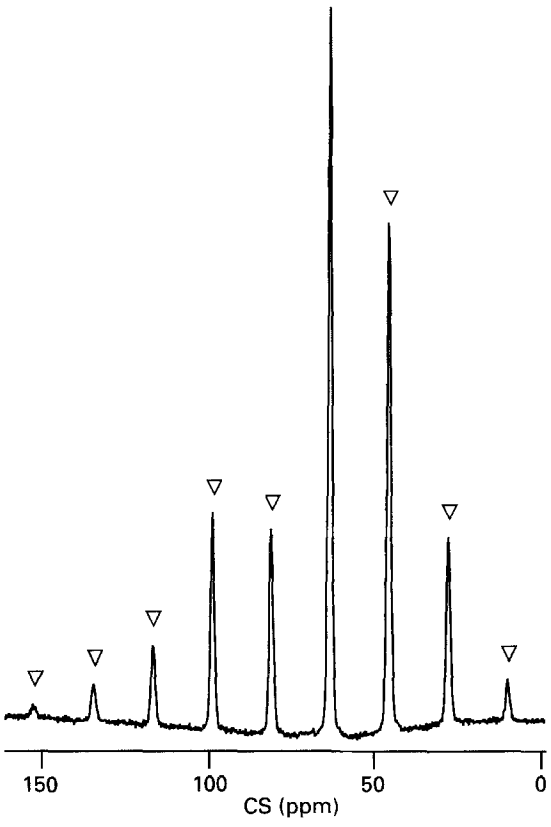

Figure 3 ^{19}F MAS NMR (sample spinning speed = 4.7 kHz; $B_0 = 6.35$ T) spectrum of crystalline synthetic fluorapatite ('▽' mark spinning sidebands).

TABLE II ^{19}F NMR chemical shift paramters in different fluorapatites (FAp) and a fluoridated hydroxyapatite (FHAp)

Sample	δ_{iso} (ppm)	$\Delta\delta$ (ppm)	η
Synthetic FAp	63.2 ± 0.5	67 ± 20	0.2 ± 0.2
FAp with heat treatment	63.0 ± 0.5	69 ± 20	0.2 ± 0.2
Synthetic FHAp	60.5 ± 0.5	47 ± 20	0.7 ± 0.3
Mineral FAp	62.6 ± 0.5	83 ± 20	0.7 ± 0.3

apatite crystals of about 1 μm in size were precipitated from the droplet phase. After being ground to a powder (particle size 1–20 μm), the apatite glass ceramic could have been used as an inorganic component in glass ionomer cements [25].

The ^{31}P MAS NMR spectrum of this glass ceramic consists of two spectral components (D,E) which clearly differ in their ^{31}P chemical shift shielding tensors and MAS linewidths (Fig. 4). Line D represents crystalline calcium apatite because of the measured ^{31}P chemical shift shielding tensor parameters and the observed MAS linewidth of 1.2 ± 0.4 ppm. The ^{19}F MAS NMR spectra lead to the conclusion that the major part of the apatite is fluorapatite (Fig. 4). The spectral component E represents a glass phase due to the MAS linewidth of 13.4 ± 0.4 ppm. The existence of isolated phosphate groups (Q^0), influenced by several cations (Na, Al, Ca), can be derived from the ^{31}P shift tensor parameters.

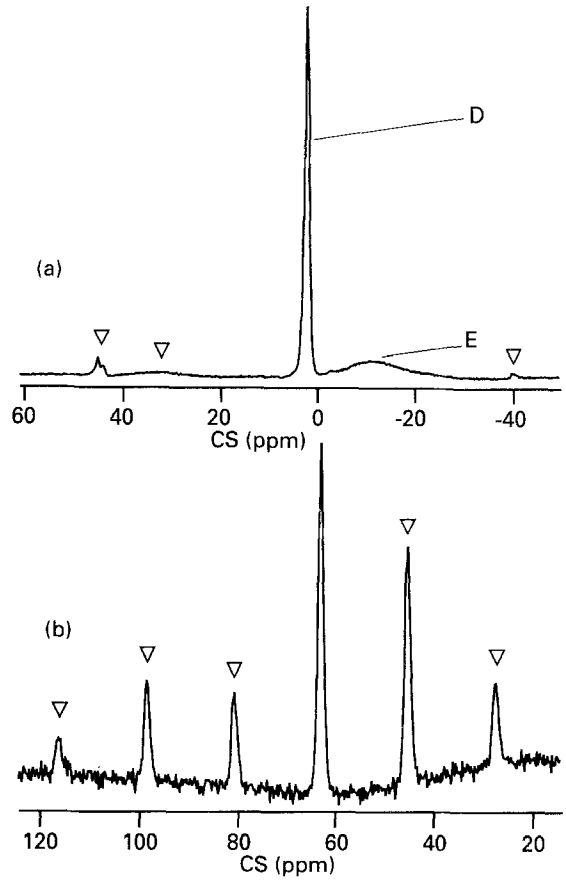

Figure 4 ^{31}P MAS NMR spectrum (a) (sample spinning speed = 4.4 kHz; $B_0 = 6.35$ T) and ^{19}F MAS NMR spectrum (b) (sample spinning speed = 4.7 kHz; $B_0 = 6.35$ T) of the apatite-containing glass ceramic ('▽' mark spinning sidebands). Line D belongs to crystalline apatite, whereas line E represents the glass phase.

4. Conclusions

The presented ^{31}P NMR investigations of various apatites show that utilization of the ^{31}P shielding tensor permits correct identification of calcium apatites contained in glasses and ceramics. The distinction between hydroxyapatite and fluoride-containing apatites is not possible due to the high structural similarity of the phosphates, whether using ^{31}P NMR (described by Haubenreißer [15]) or X-ray diffraction.

In addition, ^{19}F high-resolution solid-state NMR investigations lead to correct distinction between various apatites.

In consideration of the fact that NMR investigations, both crystalline and amorphous substances, are possible, the high-resolution solid-state NMR is an excellent tool for the analysis of glass ceramics.

References

1. U. GROSS and V. STRUNZ, in Symposium of the European Society of Biomaterials, West Berlin, 1983.
2. T. KOKUBO, in XVI International Congress on Glass, Madrid, 1992 Vol. 1, p. 119.
3. M. OKAZAKI, T. AOBA, Y. DOI, J. TAKAHASHI and Y. MORIWAKI, *J. Dent. Res.* **60** (1981) 845.
4. L. HELING, R. HEINDL and B. MERIN, *J. Oral Implantol.* **9** (1981) 548.
5. S. D. DAVIS, D. F. GIBBONS, R. L. MARTIN, S. R. LEVITT, I. SMITH and R. V. HARRINGTON, *J. Biomed. Mater. Res.* **6** (1972) 425.

6. E. LUGSCHEIDER, T. WEBER and M. KNEPPER, in NTS Conference, Cincinatti, 1988.
7. W. J. A. DHERT, *ESB News* **1** (1992) 4.
8. W. J. A. DHERT, C. P. A. T. KLEIN, J. G. C. WOLKE, E. A. VAN DER VELDE, K. DE GROOT and P. M. ROZING, *J. Biomed. Mater. Res.* **25** (1991) 1183.
9. J. HERZFELD and A. E. BERGER, *J. Chem. Phys.* **73** (1980) 6021.
10. D. FENZKE, B. MAESS and H. PFEIFER, *J. Mag. Resonance* **88** (1990) 172.
11. D. EHRT and C. JÄGER, *Z. Phys. Chem. Neue Folge* **159** (1988) 89.
12. E. J. DUFF, *Chem. Ind. (London)* **8** (1974) 349.
13. G. PIETZKA and R. EHRLICH, *Z. Analyt. Chemie* **133** (1951) 84.
14. U. HAEBERLEN, in "High resolution NMR spectroscopy in solids selective averaging" (Academic Press, New York, San Francisco, London, 1976).
15. U. HAUBENREISSER, Habilitation thesis, FSU Jena (1986).
16. A. R. GRIMMER, in Proceedings of XXth Congress Ampere, Tallinn, 1978, p. 483.
17. A. R. GRIMMER, *Spectrochimica Acta* **34A** (1978) 941.
18. T. M. DUNCAN and D. C. DOUGLASS, *Chem. Phys.* **87** (1984) 339.
19. G. L. TURNER, K. A. SMITH, R. J. KIRKPATRICK and E. OLDFIELD, *J. Mag. Resonance* **70** (1986) 2637.
20. A. NEBELUNG and M. VOGT, *Sprechsaal* **119** (1986) 566.
21. S. NARAY-SZABO, *Z. Krist.* **75** (1930) 387.
22. M. I. KAY and R. A. YOUNG, *Nature* **204** (1964) 1050.
23. K. SUDARSANAN and R. A. YOUNG, *Acta Crystallog.* **B34** (1978) 1401.
24. C. JANA and W. HÖLAND, *Silic. Ind.* **56** (1991) 215.
25. C. JANA, W. GÖTZ, G. CARL, P. WANGE, J. VOGEL and W. HÖLAND, in Transactions of the Fourth World Biomaterials Congress, Berlin, 1992, p. 515.

Received 4 August 1993
and accepted 7 April 1994